

## Measurement of the cross section for charge transfer into the states H(3s) and H(4s) for H<sup>+</sup> and D<sup>+</sup> incident on H<sub>2</sub>, N<sub>2</sub>, and O<sub>2</sub><sup>†</sup>

D. H. Loyd and H. R. Dawson

*Department of Physics, Angelo State University, San Angelo, Texas 76901*

(Received 5 August 1974)

The energy dependence of the cross section for charge transfer into the H(3s) and H(4s) states for H<sup>+</sup> and D<sup>+</sup> incident on H<sub>2</sub>, N<sub>2</sub>, and O<sub>2</sub> exhibits deviation from the form  $\sigma = A e^{-Ka|\Delta E|/hv}$  predicted by the adiabatic criterion in the range 1.2–8.2 keV. Analysis of the present data and other previously reported cross sections for protons incident on Ar, He, and Ne reveal some secondary maxima in the 2s, 3s, and 4s cross sections. Correlations between the structure in these cross sections and maxima in the total and 2p cross sections suggest intermediate-state coupling as an explanation for the observed structure.

### INTRODUCTION

Considerable effort has gone into the theoretical and experimental determination of nonsymmetrical charge-transfer collisions between ions and atoms.<sup>1–16</sup> The fundamental goal of this work has been an understanding of the dependence of the cross section upon the relative approach velocity of the colliding systems. If the ions and atoms approach one another so slowly that the state of the internal motion is able to adjust itself to the perturbation, the probability of transition is small. This is the “adiabatic criterion” described by Massey.<sup>9,10,15</sup> Conditions can be considered to be adiabatic when

$$a|\Delta E|/hv \gg 1, \quad (1)$$

where  $\Delta E$  (eV) is the energy defect for the process,  $v$  is the relative velocity of approach, and  $a$  (in Å) is a parameter of the order of the atomic dimensions involved.

It has been proposed that the cross section should exhibit the following behavior: (a) In the adiabatic region it should have the form

$$\sigma = A e^{-Ka|\Delta E|/hv}, \quad (2)$$

where  $A$  and  $K$  are constants; (b) the termination of the adiabatic region for proton impact is marked by

$$V_m = a^2|\Delta E|^2/324, \quad (3)$$

where  $V_m$  (keV) is the impact energy at maximum cross section; (c) beyond the region of the maximum, the cross section should decrease rapidly as the energy increases.<sup>9,10,15</sup>

The experimental results of several investigators have shown much better agreement in general with the second and third predictions than with the first.<sup>1–4,11,13</sup> In particular, it has been found that the energy of the experimentally determined maxi-

mum in the cross section is predicted quite well by Eq. (3) with a value for the adiabatic parameter given by  $a = 7 \text{ \AA}$ .<sup>16</sup>

Charge-exchange cross sections at energies less than the energy for the cross-section maximum have been of particular interest because they exhibit an oscillatory behavior for certain interactions in contradiction to the first prediction. The present experiment examines an energy range below the energy of the observed maximum in the cross section for electron capture into the 3s and 4s states of H by fast-proton impact on H<sub>2</sub>, N<sub>2</sub>, and O<sub>2</sub>.

### APPARATUS AND PROCEDURE

Techniques used for the cross-section measurements are described in Refs. 1, 3, and 4 and a detailed description of the apparatus is contained in Ref. 3. The experimental procedure was identical to that in Ref. 3 and can be summarized as follows.

A monoenergetic proton (or deuteron) beam was passed through the target gas in a differentially pumped collision chamber. Gas pressures were set in the collision chamber so that the beam attenuation was approximately 10%.

A beam which emerged from the collision chamber into an evacuated observation chamber was partially composed of atomic hydrogen in the 3s and 4s states resulting from charge-exchange collisions between protons and the target gas. Photon emission intensity (per unit beam current), owing to the decay of these excited states, was measured as the beam passed through the observation chamber. The proton (or deuteron) flux was measured at a Faraday cup and corrected for neutralization inside the collision and observation chambers.

Cross sections for capture into the 3s state were determined by measuring the intensity of the radiation in the 3s → 2p transition of the H<sub>α</sub> ( $n = 3 \rightarrow 2$ )

TABLE I. Cross section in units of  $10^{-19}$  cm<sup>2</sup>.

H <sup>+</sup> energy <sup>a</sup> (keV)	Hydrogen		Nitrogen		Oxygen	
	3s	4s	3s	4s	3s	4s
1.2	3.7 ± 0.7	0.96 ± 0.05	...	3.5 ± 0.3	...	...
1.7	3.7 ± 0.8	1.05 ± 0.03	24.4 ± 0.6	4.2 ± 0.2	25.8 ± 0.6	4.04 ± 0.10
2.2	5.6 ± 0.7	1.42 ± 0.17	25.1 ± 0.8	6.3 ± 0.1	31.5 ± 2.8	4.06 ± 0.14
2.7	8.2 ± 1.1	1.67 ± 0.11	29.8 ± 0.8	6.7 ± 0.2	30.7 ± 3.3	5.02 ± 0.16
3.2	8.1 ± 0.6	1.77 ± 0.21	33.7 ± 1.0	7.6 ± 0.3	36.2 ± 6.5	4.57 ± 0.86
4.2	8.9 ± 0.3	2.18 ± 0.18	36.4 ± 0.7	9.2 ± 0.5	41.9 ± 3.3	6.35 ± 0.36
5.2	10.5 ± 0.1	2.46 ± 0.10	35.2 ± 0.3	9.8 ± 0.1	49.2 ± 7.2	6.31 ± 0.14
6.2	11.9 ± 0.9	2.80 ± 0.06	37.7 ± 0.2	10.3 ± 0.2	42.8 ± 2.1	6.78 ± 0.14
7.2	13.4 ± 0.9	2.91 ± 0.04	38.7 ± 0.4	10.5 ± 0.1	44.9 ± 5.8	6.23 ± 0.11
8.2	16.0 ± 0.1	3.11 ± 0.04	42.0 ± 0.1	11.5 ± 0.3	48.0 ± 2.9	7.00 ± 0.07

<sup>a</sup>Deuteron data listed at proton energy having same particle velocity as deuteron energy used.

line. Other transitions in the H<sub>α</sub> radiation made essentially no contribution since the H<sub>α</sub> intensity was measured at a point sufficiently far from the collision chamber to ensure that the relatively short-lived 3*p* and 3*d* states were no longer populated.

The same technique was applied to the 4*s* cross-section measurements where the relatively long 4*s* lifetime allows separation of the 4*s* → 2*p* transition from others in the H<sub>β</sub> (*n* = 4 → 2) line.

Analysis of the data produced relative cross-section values. Absolute values for the cross section were determined by normalizing the relative values to published values for the absolute cross sections at 5 keV and above.<sup>1</sup>

Using protons as incident particles, measurements were made in 1-keV steps between 3.2 and 8.2 keV. Using deuterons as incident particles, measurements were made at impact velocities equivalent to proton energies of 1.2, 1.7, 2.2, 2.7, 3.2, and 4.2 keV.

## RESULTS AND DISCUSSION

Graphs of the data tabulated in Table I are shown in Figs. 1–3. The error bars show the standard deviation from the mean of several trials and represent the reproducibility which typically was within 10%. Factors restricting reproducibility were poor signal-to-noise ratio, fluctuations in target-gas pressure and beam current, and short-term electronic drift.

Figure 1 shows log-log plots of the present measurements of the 3*s* and 4*s* cross sections versus energy for proton and deuteron impact on H<sub>2</sub>. Also shown are previous measurements by Hughes *et al.*<sup>1</sup> of the 3*s* and 4*s* cross sections as well as the measurements by Bayfield<sup>2</sup> of the 2*s* cross section. The general features of the cross-section curves for all three processes show a great deal

of similarity above 10 keV. Below 10 keV there is less similarity in the curve shapes, with the 2*s* curve showing somewhat better evidence of secondary structure.

Figure 2 shows log-log plots of the present measurements of the 3*s* and 4*s* cross sections versus energy for proton and deuteron impact on N<sub>2</sub>. Also shown are the measurements of Hughes *et al.*<sup>1</sup> of these cross sections at higher energies. The 3*s*

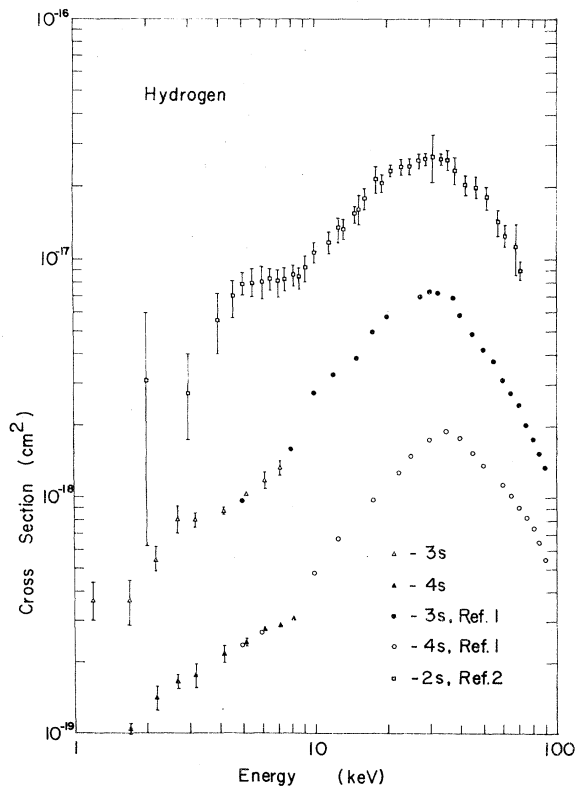


FIG. 1. Plot of 3*s* and 4*s* capture by H<sup>+</sup> and D<sup>+</sup> on H<sub>2</sub>. Also shown are the data of Refs. 1 and 2.

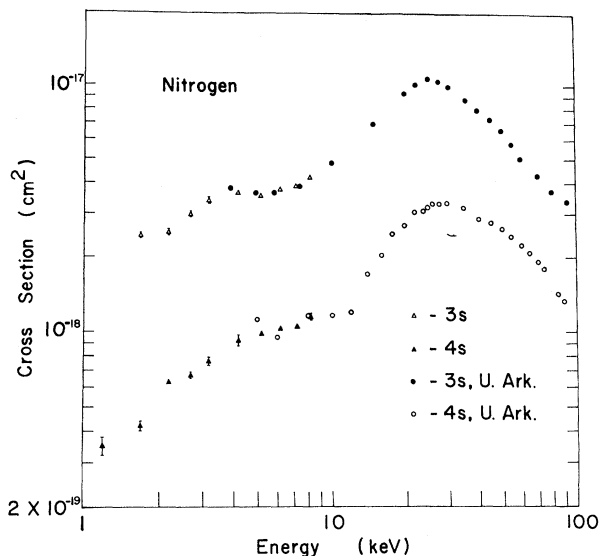


FIG. 2. Plot of 3s and 4s capture by  $H^+$  and  $D^+$  on  $N_2$ . Also shown are the data of Ref. 1.

cross section shows a definite indication of a secondary peak in the vicinity of 4 keV. The 4s cross section seems to level off in the vicinity of 5 keV but does not show a resolved secondary maximum.

Figure 3 shows log-log plots of the 3s and 4s cross sections versus energy for protons and deuterons incident upon  $O_2$ . The general shape of the 3s cross section is the most complex of all the cross sections examined in this experiment. In the high-energy region Hughes *et al.*<sup>1</sup> have noted the existence of two peaks; one about 15 keV and

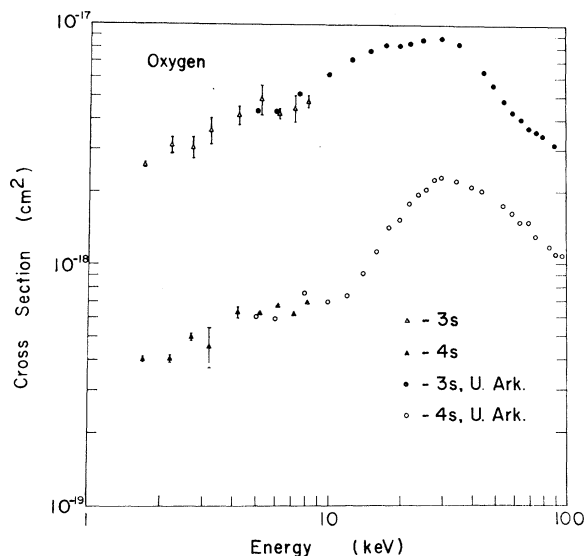


FIG. 3. Plot of 3s and 4s capture by  $H^+$  and  $D^+$  on  $O_2$ . Also shown are the data of Ref. 1.

the other near 30 keV. In the energy region investigated by the present experiment there is some indication of a peak near 5 keV. The 4s cross section, which is similar to the other cross sections, shows a peak around 30 keV and a rather flat region below 10 keV.

The general shapes and over-all magnitudes of the cross sections measured in this experiment and those from Ref. 3 are compared in Figs. 4 and 5. Both the 3s and 4s cross sections allow the same general kind of comparison. The cross section for impact on He is the smallest of the six gases shown. All the cross sections for impact on Ar,  $O_2$ ,  $N_2$ , and Kr are about the same and are about a factor of 10 larger than the cross section for impact on He. The magnitude of the cross section for impact on  $H_2$  is about halfway between that for He and for the other four gases.

The adiabatic criterion predicts that below the maximum the cross section will vary as Eq. (2). Using the data of Refs. 1-4 and 13, a least-squares fit to Eq. (2) was attempted in the region immediately below the cross-section maximum. The cross sections involved were the 3s and 4s cross sections

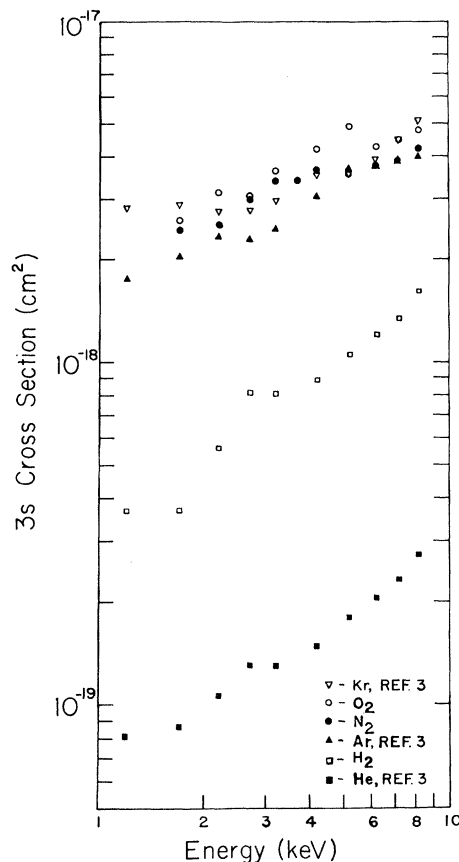


FIG. 4. Plot of 3s capture by  $H^+$  and  $D^+$  on six target gases.

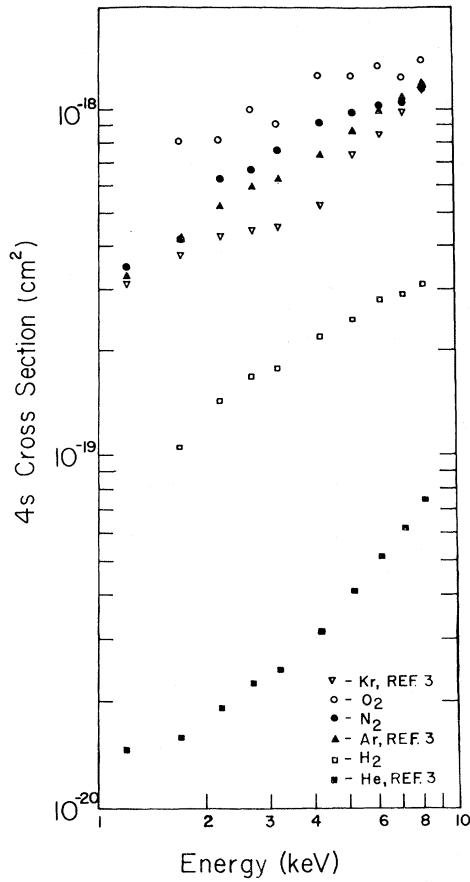


FIG. 5. Plot of 4s capture by  $H^+$  and  $D^+$  on six target gases.

for proton impact on  $H_2$ ,  $N_2$ ,  $O_2$ , Ne, He, and Ar and the 2s cross section for proton impact on  $H_2$ , He, and Ne. The solid curves shown in Fig. 6 are the results of these fits for  $H_2$ ,  $N_2$ , and  $O_2$  and are typical of the results for the 15 cross sections fitted. For the points above 10 keV but below the maximum the correlation coefficients for the least-squares fits were between 0.986 and 0.999. An examination of the parameter  $K$  in Eq. (2) shows that its variation for these 15 different curves is such that an average is given by  $K = 1.60 \pm 0.43$ , assuming the value of  $a = 7 \text{ \AA}$ . The variation in  $K$  to fit the curve shapes is therefore about 27%, which is of the same order as the 20% variation of the adiabatic parameter determined from Eq. (3) using experimental values for the energy of the cross-section maximum. Therefore, down to around 10 keV, Eq. (2) (with  $K = 1.60 \pm 0.43$ ) describes the shape of the cross section approximately as well as the location of the cross-section maximum is predicted by Eq. (3) (with  $a = 7.0 \pm 1.4 \text{ \AA}$ ).

It is clear that in the region between 1 and 10 keV an extension of the solid curve described above does not predict the behavior of the cross section. In every case there appears to be a definite change in the slope of the curve and in some cases even an indication of a secondary maximum. A possible interpretation of the shape of the curve might be that there are two broad maxima in the cross section with the high-energy peak being the largest. The secondary peak would then be obscured by the interference between the two peaks in the region between them.

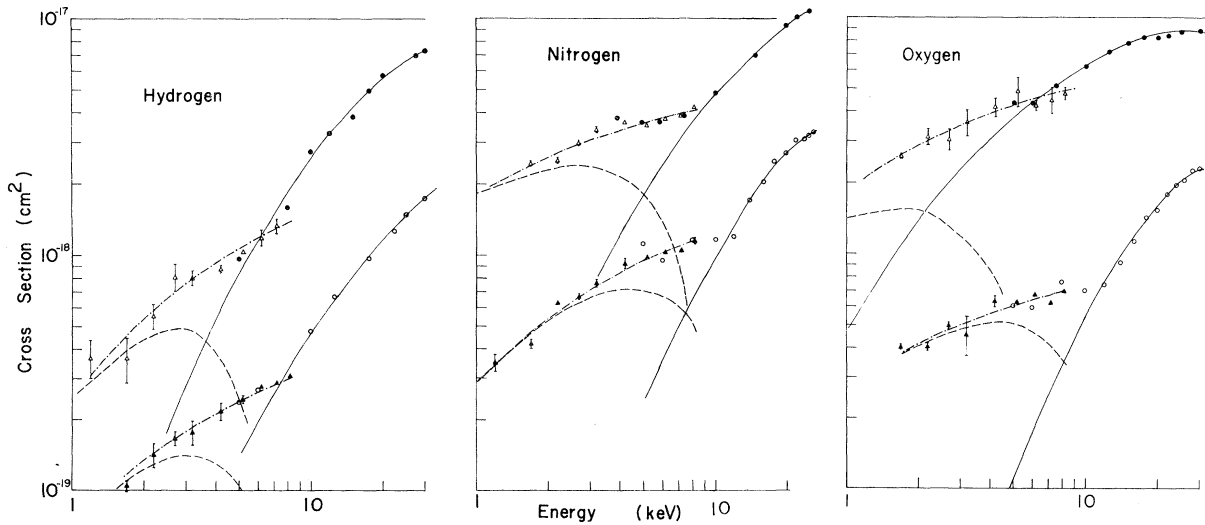


FIG. 6. Plot of cross-section data from Table I and Ref. 1.  $\Delta$ , 3s capture data from Table I;  $\blacktriangle$ , 4s capture data from Table I;  $\bullet$ , 3s capture data from Ref. 1;  $\circ$ , 4s capture data from Ref. 1; solid line, least-squares fit of Eq. (2) to data below maximum in cross section; dash-dot line, smooth-curve fit to data from Table I; dashed line, curve obtained by subtracting Eq. (2) from the smooth curve.

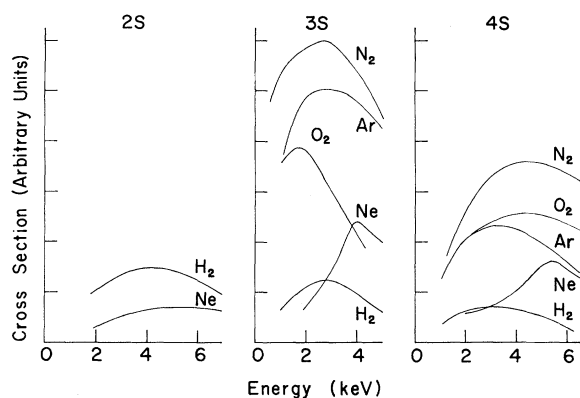


FIG. 7. Plot showing 12 cross-section maxima obtained by subtraction. 2s, 3s, and 4s capture by  $H^+$  and  $D^+$  on He produced no maxima in this energy range and are therefore not shown.

If indeed two peaks are present, they can be resolved if the following assumptions are made: (i) The contribution from the major peak is that predicted by extending the fit above 10 keV to the region below 10 keV (solid curve); (ii) a smooth curve can be fitted to the actual data in the region between 1 and 10 keV (dot-dashed curve). With these

two assumptions the contribution from the secondary peak is then found as the difference between actual data and the contribution from the major peak (dashed curve).

Figure 6 shows the results of such a procedure for six of the cross-section curves which are typical of the results of the process. Figure 7 shows a graph of the curve shapes on a linear scale for the 12 cross sections for which a secondary peak does result from this analysis. No secondary structure resulted from the He analysis. If the secondary maxima resulting from the above analysis are indeed real, one might expect to find explanations for them in the coupling to other states during the collision process.<sup>13</sup> For example, if coupling between the ground state and excited states is significant, one would expect a correlation between the  $H(nl)$  cross-section maxima and the total cross-section maxima. Such a correlation does exist for the excited-state cross sections for impact on  $N_2$  and Ar. The same correlation for  $H_2$  and Ne exists for certain published values but not for others (see Table II). Another correlation exists between  $ns$ -state cross sections and the  $2p$  cross sections for impact on Ne and Ar, indicating possible  $p$ - $s$  state mixing during the colli-

TABLE II. Energy of cross-section maximum (nearest keV) below 10 keV as determined from curves shown in Fig. 7. Also shown are maxima for possibly related reactions discussed in the text.

Reaction	$V_m$ (keV) from Fig. 7	$V_m$ (keV) from indicated Ref.
$H^+ + H_2 \rightarrow \sum H(nl) + H_2^+$		3 (Ref. 17), 7 (Ref. 2)
$H^+ + H_2 \rightarrow H(2s) + H_2^+$	4	
$H^+ + H_2 \rightarrow H(3s) + H_2^+$	3	
$H^+ + H_2 \rightarrow H(4s) + H_2^+$	3	
$H^+ + N_2 \rightarrow \sum H(nl) + N_2^+$		4 (Ref. 18)
$H^+ + N_2 \rightarrow H(3s) + N_2^+$	3	
$H^+ + N_2 \rightarrow H(4s) + N_2^+$	4	
$H^+ + O_2 \rightarrow \sum H(nl) + O_2^+$		unknown
$H^+ + O_2 \rightarrow H(3s) + O_2^+$	2	
$H^+ + O_2 \rightarrow H(4s) + O_2^+$	5	
$H^+ + Ne \rightarrow \sum H(nl) + Ne^+$		7 (Ref. 14), 11 (Ref. 17)
$H^+ + Ne \rightarrow H(2s) + Ne^+$	6	
$H^+ + Ne \rightarrow H(3s) + Ne^+$	4	
$H^+ + Ne \rightarrow H(4s) + Ne^+$	6	
$H^+ + Ne \rightarrow H(2p) + Ne^+$		6 (Ref. 13)
$H^+ + Ar \rightarrow \sum H(nl) + Ar^+$		2 (Ref. 13), 3 (Ref. 2), 4 (Ref. 17)
$H^+ + Ar \rightarrow H(3s) + Ar^+$	3	
$H^+ + Ar \rightarrow H(4s) + Ar^+$	3	
$H^+ + Ar \rightarrow H(2p) + Ar^+$		4 (Ref. 13)
$H^+ + He \rightarrow \sum H(nl) + He^+$		no max. (Refs. 13, 17)
$H^+ + He \rightarrow H(2s) + He^+$	no max.	
$H^+ + He \rightarrow H(3s) + He^+$	no max.	
$H^+ + He \rightarrow H(4s) + He^+$	no max.	
$H^+ + He \rightarrow H(2p) + He^+$		no max. (Ref. 13)

sion process. The significance of these correlations is supported by the fact that analysis of 2s, 3s and 4s cross sections for impact on He revealed no secondary structure below 10 keV, while the 2p and total cross sections also show no maxima in this energy range.

## ACKNOWLEDGMENTS

We wish to thank Kelly Knowlton and Barbara Nibling for their able assistance in taking the data and R. H. Hughes for his critical reading of the manuscript.

†This research was supported by the Robert A. Welch Foundation.

<sup>1</sup>R. H. Hughes, H. R. Dawson, and B. M. Doughty, *Phys. Rev.* **164**, 166 (1967).

<sup>2</sup>J. E. Bayfield, *Phys. Rev.* **182**, 115 (1969).

<sup>3</sup>H. R. Dawson and D. H. Loyd, *Phys. Rev. A* **9**, 166 (1974).

<sup>4</sup>R. H. Hughes, H. R. Dawson, B. M. Doughty, D. B. Kay, and C. A. Stigers, *Phys. Rev.* **146**, 53 (1966).

<sup>5</sup>J. R. Oppenheimer, *Phys. Rev.* **31**, 349 (1928).

<sup>6</sup>J. D. Jackson and H. Schiff, *Phys. Rev.* **89**, 359 (1953).

<sup>7</sup>D. R. Bates and A. Dalgarno, *Proc. Phys. Soc. Lond. A* **66**, 972 (1953).

<sup>8</sup>D. Rapp and W. E. Francis, *J. Chem. Phys.* **37**, 2631 (1962).

<sup>9</sup>H. S. W. Massey, *Rep. Prog. Phys.* **12**, 248 (1949).

<sup>10</sup>H. S. W. Massey and E. H. S. Burhop, *Electronic and*

*Ionic Impact Phenomena* (Clarendon, Oxford, England, 1952), pp. 513 and 514.

<sup>11</sup>S. Dworetsky, R. Novick, W. W. Smith, and N. Tolk, *Phys. Rev. Lett.* **18**, 939 (1967).

<sup>12</sup>R. A. Mapleton, *Phys. Rev.* **122**, 528 (1961).

<sup>13</sup>D. Jaecks, B. Van Zyl, and R. Geballe, *Phys. Rev.* **137**, A340 (1965).

<sup>14</sup>J. B. Hasted and J. B. H. Stedeford, *Proc. R. Soc. A* **277**, 466 (1955).

<sup>15</sup>J. B. Hasted and A. R. Lee, *Proc. Phys. Soc. Lond.* **79**, 702 (1962).

<sup>16</sup>J. B. Hasted, *Physics of Atomic Collisions* (American Elsevier, New York, 1972), pp. 623 and 624.

<sup>17</sup>S. K. Allison, *Rev. Mod. Phys.* **30**, 1137 (1958).

<sup>18</sup>J. S. Murray, S. J. Young, and J. R. Sheridan, *Phys. Rev. Lett.* **16**, 439 (1966).